Experimental demonstration of revival of oscillations from death in coupled nonlinear oscillators

D. V. Senthilkumar, K. Suresh, V. K. Chandrasekar, Wei Zou, Syamal K. Dana, Thamilmaran Kathamuthu, and Jürgen Kurths

Citation: Chaos **26**, 043112 (2016); doi: 10.1063/1.4947081
View online: http://dx.doi.org/10.1063/1.4947081
View Table of Contents: http://scitation.aip.org/content/aip/journal/chaos/26/4?ver=pdfcov
Published by the AIP Publishing

Experimental demonstration of revival of oscillations from death in coupled nonlinear oscillators

D. V. Senthilkumar,[1,2,a)] K. Suresh,[3,4] V. K. Chandrasekar,[2] Wei Zou,[5,6] Syamal K. Dana,[7] Thamilmaran Kathamuthu,[4] and Jürgen Kurths[8,9,10,11]
[1]*School of Physics, Indian Institute of Science Education and Research, Thiruvananthapuram 695016, India*
[2]*Centre for Nonlinear Science and Engineering, School of Electrical and Electronics Engineering, SASTRA University, Thanjavur 613 401, India*
[3]*Department of Physics, Anjalai Ammal-Engineering College, Kovilvenni 614 403, Tamilnadu, India*
[4]*Centre for Nonlinear Dynamics, Bharathidasan University, Trichy 620024, Tamilnadu, India*
[5]*School of Mathematics and Statistics, Huazhong University of Science and Technology, Wuhan 430074, China*
[6]*Centre for Mathematical Sciences, Huazhong University of Science and Technology, Wuhan 430074, China*
[7]*CSIR-Indian Institute of Chemical Biology, Kolkata 700032, India*
[8]*Potsdam Institute for Climate Impact Research, Telegrafenberg, Potsdam D-14415, Germany*
[9]*Institute of Physics, Humboldt University Berlin, Berlin D-12489, Germany*
[10]*Institute for Complex Systems and Mathematical Biology, University of Aberdeen, Aberdeen AB24 3FX, United Kingdom*
[11]*Department of Control Theory, Nizhny Novgorod State University, Gagarin Avenue 23, 606950 Nizhny Novgorod, Russia*

(Received 4 December 2015; accepted 5 April 2016; published online 22 April 2016)

We experimentally demonstrate that a processing delay, a finite response time, in the coupling can revoke the stability of the stable steady states, thereby facilitating the revival of oscillations in the same parameter space where the coupled oscillators suffered the quenching of oscillation. This phenomenon of reviving of oscillations is demonstrated using two different prototype electronic circuits. Further, the analytical critical curves corroborate that the spread of the parameter space with stable steady state is diminished continuously by increasing the processing delay. Finally, the death state is completely wiped off above a threshold value by switching the stability of the stable steady state to retrieve sustained oscillations in the same parameter space. The underlying dynamical mechanism responsible for the decrease in the spread of the stable steady states and the eventual reviving of oscillation as a function of the processing delay is explained using analytical results. *Published by AIP Publishing*. [http://dx.doi.org/10.1063/1.4947081]

Oscillation quenching is such a fascinating emerging behavior, whereby the interaction between oscillatory units ceases the oscillations to exist. Phenomenologically, amplitude death (AD) and oscillation death (OD) have been clearly distinguished as two distinct types of oscillation quenching. The mechanisms which have the tendency to induce oscillation quenching are prevalent in many natural systems. However, in various realistic circumstances, several phenomena very often involve oscillations, and hence, the quenching of oscillations in many natural systems is undesirable, which needs to be circumvented for their sustained evolution. In addition, despite the ubiquity of the conditions conducive to the onset of AD/OD, several natural systems retain their sustained oscillations. For instance, internet can fail for some finite time after a severe attack and then, after a period of time, recover. A human brain is capable of recovering spontaneously after an epileptic attack. A traffic network returns to its normal state after a period of gridlock. A financial network may, after a period of time, recover after having a large fraction of its constituents fail. Thus, it is also inevitable to unravel the underlying dynamical mechanisms that are responsible for the sustained oscillations of many natural systems and manmade networks. Here, we will demonstrate experimentally using two different prototype nonlinear electronic circuits that their natural dynamics can be revived, after their dynamical activity ceases to exist irreversibly, by the introduction of a processing delay in the coupling. Further, our analytical results clearly reveal the dynamical mechanisms of the curtailing effect of the processing delay on the spread of AD/OD regions, which finally result in the reviving of oscillations in the AD/OD regions above a threshold value of the processing delay.

Coupled nonlinear oscillators have been extensively employed in understanding various complex collective phenomena in diverse natural systems.[1–5] Quenching of oscillations[6,7] is such an emergent behavior in coupled oscillators, where the oscillators drive each other to stable equilibrium/equilibria under coupling. This phenomenon was evidenced first as an unexpected silencing of two side-by-side organ pipes[8] and was later observed in chemical reactions,[9] neural oscillators,[10] lasers,[11] electronic circuits,[12,13] etc. Phenomenologically, two distinct classes of oscillation quenching have been classified—amplitude death (AD) and oscillation death (OD)—depending on whether the coupled oscillators populate the homogeneous steady state (HSS) or

a)Electronic mail: skumarusnld@gmail.com

the different branches of the inhomogeneous steady state (IHSS), respectively. Recent investigations are centered at the identification of AD-OD transitions.[14–18] Despite a few applications of AD/OD,[19–21] their onset deteriorates the degree of performance of several real world systems, where sustained oscillations should be retained for their evolution, and can result in cascading failures leading to a complete collapse, for instance, extinction of species in ecological network, gridlock in traffic network, market crashes in financial network, and a large-scale power blackout. Hence, the emergence of AD/OD in such systems should be evaded in their own parameter space despite prevalence of the conditions conducive to their onset.

Efforts have been made to revive oscillations of the coupled networks after their dynamic activities cease to exist irreversibly.[22–25,27] Recently, a processing delay, a finite time required to process the information received at the interface, in the coupling is shown to effectively annihilate the onset of AD/OD.[25] This is in sharp contrast with the effect of propagation delay, a finite time required for the signal propagation from one node to the other due to their spatial separation, which has the tendency to induce AD[26] in coupled identical oscillators. Thus, the processing delay can compete with the quenching effects of the propagation delay in switching the stability of the stable steady states above a critical value. Indeed, it was clearly shown that, in Ref. 25, the processing delay is capable of retrieving the oscillations from the AD state induced by the propagation delay.[26] It is interesting to note that the effect of processing delay is counter-intuitive to the quenching effects of the propagation delay. Signals/information in almost all technological networks such as computer server, communication networks, traffic networks, automated logistic networks, and routers are processed essentially by appropriate oscillatory circuits. In particular, in neuroscience, the electronic-neural cell hybrids have been used to investigate the collective behavior of neural oscillators, such as central pattern generators.[28] As the emergence of AD/OD in such circuit systems is not always desirable for their proper functioning, experimental realization of the reviving of oscillations in the AD/OD parameter space using electronic circuit systems is of vital importance because of their immense potential applications.

In this paper, we will experimentally demonstrate that the processing delay in the coupling can annihilate the onset of AD/OD by switching the stability of the stable HSS (AD) and IHSS (OD) using analog electronic circuits of van der Pol (VDP) oscillators exhibiting limit-cycle oscillations and Sprott systems representing chaotic oscillators. Recently, diverse bifurcation scenarios pertaining to the transition from AD to OD in these systems are unveiled under repulsive links.[16] We consider the same parameter space of the AD-OD transitions in the two coupled VDP and Sprott oscillators, respectively, to experimentally demonstrate that the processing delay can effectively evoke oscillations from both AD and OD regions. First, we consider two diffusively coupled VDP oscillators[16]

$$\dot{x}_i = y_i - \varepsilon_i(x_j(t-\delta) + x_i(t-\delta)), \tag{1a}$$

$$\dot{y}_i = b(1-x_i^2)y_i - x_i + \varepsilon(y_j(t-\delta) - y_i(t-\delta)), \tag{1b}$$

where $i,j = 1,2$, $i \neq j$, b is the system parameter, $\varepsilon = \varepsilon_1$ is the coupling strength, $\varepsilon_2 = 0$ represents the unidirectional repulsive link, and δ is the processing delay, which is the time taken by the node y_1 to process the information y_2 reached y_1 prior by δ and vice versa in the diffusive coupling. We have fixed $N = 2$ in our present investigation. The analog electronic circuit of the coupled VDP oscillators (1) and the corresponding dynamical equations are provided in Ref. 30. For $\varepsilon = 0$, the origin is the unstable fixed point of each VDP oscillator exhibiting limit-cycle oscillations. The coupled VDP oscillators, Eq. (1), have two fixed points $x_1^* = \pm\sqrt{1-\frac{1}{b\varepsilon}}, y_1^* = \varepsilon\frac{\sqrt{1-\frac{1}{b\varepsilon}}}{1-\varepsilon^2}, x_2^* = \varepsilon y_1^*, y_2^* = 0$ besides the origin. The origin is the HSS, where both oscillators populate resulting in AD for appropriate coupling, while the other two fixed points contribute to the IHSS, where the two oscillators populate the different branches of the IHSS resulting in OD for suitable ε.

Snapshots of the evolution of the coupled VDP oscillators, as observed experimentally in the oscilloscope, are depicted in Fig. 1 for $b = 0.5$. The stable HSS is seen in Fig. 1(a) for $\varepsilon = 1.0$ until the processing delay $\delta = 0$. Now, as soon as a finite processing delay $\delta = 0.5 > \delta_c$ is switched on, indicated by the arrow, the oscillations of both the VDP oscillators in (1) are retrieved for the same parameters (see Fig. 1(a)) after initial transients. For $b = 0.5$, the transition

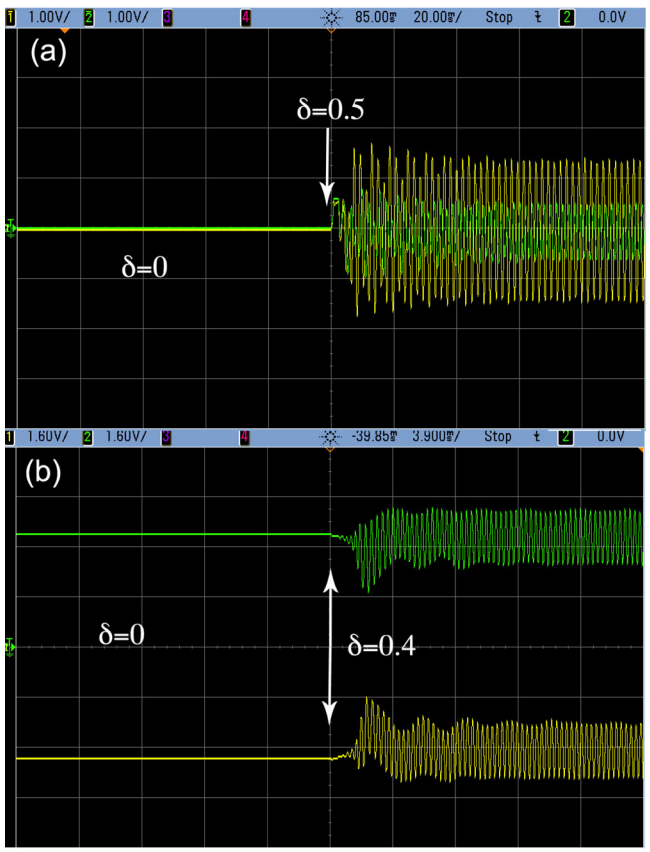

FIG. 1. Real time traces of the coupled VDP oscillators (1) depicting the reviving of oscillation from the stable (a) HSS for $b = 0.5, \varepsilon = 1.0$, and $\delta = 0.5$, and (b) IHSS for $b = 0.5, \varepsilon = 2.5$, and $\delta = 0.4$. In both figures, as soon as a finite processing delay $\delta > \delta_c$ is switched on, indicted by the arrow, the oscillations are retrieved from both the AD and OD states.

from AD to OD occurs at the critical coupling strength $\varepsilon_c = 2.0$ via a pitchfork bifurcation (see Fig. 2). The existence of the stable IHSS is clearly visualized in Fig. 1(b) for $\varepsilon = 2.5$ until $\delta = 0$, and the oscillations are revived immediately as soon as an appropriate processing delay $\delta = 0.4$ is introduced.

The dynamics of the coupled VDP oscillators observed experimentally in a range of the system parameter $b \in (0, 1)$ and the coupling strength $\varepsilon \in (0, 3)$ depicting the spread of the stable HSS (checked region) and the stable IHSS (filled region) is shown in Fig. 2(a) for different values of the processing delay δ. The entire checked and the filled area corresponds to AD and OD, respectively, for $\delta = 0$, while the empty space corresponds to oscillatory regimes. It is clearly evident from Fig. 2(a) that the spread of AD/OD rapidly decreases upon increasing the processing delay and eventually erased completely above δ_c resulting in the revival of oscillations in the AD/OD parameter space by switching the stability of the stable HSS/IHSS. The OD region is wiped off above $\delta_c = 0.34$, while the stable HSS completely losses it stability above $\delta_c = 0.46$. Thus, the presence of even a small processing delay is capable of overcoming the quenching effects in retaining the sustained oscillations of the coupled systems.

By performing a linear stability analysis around the fixed points, for $\delta = 0$, the stability condition for the HSS to be stable is obtained as $b < \varepsilon < \frac{1}{b}$, while that for the IHSS to be stable is $\frac{1}{b} < \varepsilon < b_c$.[29] In the presence of δ, the characteristic equation of the coupled VDP oscillators, Eq. (1), corresponding to the fixed point at the origin can be written as $(1 - b\lambda + 2\varepsilon e^{-\lambda\delta}\lambda + \lambda^2)(1 + \varepsilon e^{-\lambda\delta}\lambda + \lambda^2 - b(\varepsilon e^{-\lambda\delta} + \lambda)) = 0$. The stability of the HSS/IHSS is changed if the eigenvalue $\lambda = \alpha + i\beta$ of the characteristic equation crosses the imaginary axis $\lambda = i\beta$. Thus, the oscillations are revived from AD/OD via a Hopf bifurcation as α surpasses zero from $\alpha < 0$. The critical stability curves $\delta_c(\varepsilon)$ of the HSS can be deduced as

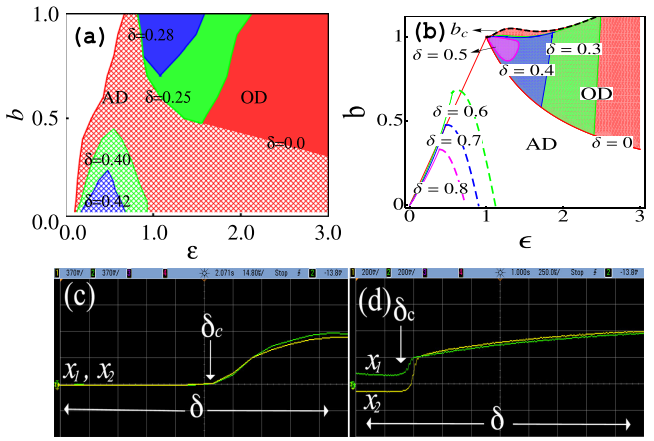

FIG. 2. Spread of the stable HSS and IHSS of the coupled VDP oscillators (1) for different values of δ as a function of the coupling strength ε and the system parameter b elucidating the effect of the processing delay δ. (a) Experimental results and (b) analytical stability curves. Real time bifurcation diagrams elucidating the revival of oscillations for $\delta > \delta_c$ from (c) HSS for $b = 0.5$ and $\varepsilon = 1.0$ for $\delta \in (0, 0.6)$ and (d) IHSS for $b = 0.5$ and $\varepsilon = 2.5$ for $\delta \in (0, 0.3)$.

$$\delta_1 = -\cos^{-1}\left(\frac{b}{2\varepsilon}\right)\left(\varepsilon\sqrt{1-\frac{b^2}{4\varepsilon^2}} + \sqrt{1+\varepsilon^2\sqrt{1-\frac{b^2}{4\varepsilon^2}}}\right),$$
$$\delta_2 = \cos^{-1}(\beta)\frac{(1-\varepsilon\beta)}{\varepsilon\sqrt{1-b^2\beta^2}}, \tag{2}$$

where $\beta = ((2 + b^2 + \varepsilon^2) - \sqrt{(b^2 + \varepsilon^2)^2 - 4(b^2 - \varepsilon^2)})(2(1 + 2b^2)\varepsilon)^{-1}$. The stability of the two other fixed points (IHSS) can be obtained by simplifying $e^{-\lambda\delta}$ in the characteristic equation using a series expansion $e^{-\lambda\delta} = \sum_{n=0}^{\infty}(-\lambda\delta)^n/n!$ for $\delta < 1$.

The analytical critical curves determining the stable HSS (region between two solid lines) and the stable IHSS (filled region) are depicted in Fig. 2(b) as functions of ε and b for different values of δ. The two solid lines at the left and the right boundary of the AD region for $\delta = 0$ correspond to $\varepsilon = b$ and $\varepsilon = \frac{1}{b}$, respectively. The uppermost boundary (thick dashed line) encompassing the stable IHSS is obtained for $b = b_c$.[29] The regions enclosed by the critical curves δ_1 (solid lines) and δ_2 (dashed lines) are the AD regions for different values of $\delta = 0, 0.6, 0.7$, and 0.8. It is evident that the spread of the AD region decreases for increasing δ until AD is completely wiped off due to change in the stability of the stable HSS, thereby regaining the oscillations. The stable IHSS for $\delta = 0, 0.3, 0.4$, and 0.5, obtained using the Routh-Hurwitz criteria, is shown in Fig. 2(b) (shaded regions), elucidating that the OD region shrinks with the increase in δ, which is also capable of switching the stability of the stable IHSS above δ_c to retain sustained stable oscillations of the coupled systems. The analytical critical curves in Fig. 2(b) corroborate the experimental observation of the effect of the processing delay in decreasing the spread of AD/OD regions and in switching the stability of the stable HSS/IHSS in the AD/OD parameter space above δ_c, thereby reviving the oscillations of the coupled VDP oscillators to retain their rhythmic behavior. In addition, the real time bifurcation diagram of the coupled VDP oscillators corroborates the revival of oscillations for $\delta > \delta_c$ from the AD state (see Fig. 2(c), where $x_{1,2}$ vs $\delta \in (0, 0.6)$ is depicted) for $b = 0.5$, $\varepsilon = 1.0$, and from the OD state for $b = 0.5$, $\varepsilon = 2.5$, as shown in Fig. 2(d) for $\delta \in (0, 0.3)$. The real time bifurcation diagram refers to the real time trace of Poincaré points in the oscilloscope using electronic circuits, as the control parameter is varied.

To gain further insights on the curtailing effect of the processing delay on the spread of the AD/OD regions below δ_c, we consider a rather general two coupled dynamical systems $\dot{x}_{1,2} = f_{1,2}(x_{1,2}) + \varepsilon(x_{2,1}(t-\delta) - x_{1,2}(t-\delta))$ each of dimension d, whose linearized equation about the steady state is represented as $\dot{\eta}_{1,2} = \mu_{1,2}\eta_{1,2} + \varepsilon(\eta_{2,1}(t-\delta) - \eta_{1,2}(t-\delta))$, where $\eta_{1,2}$ denotes the dynamics of the perturbation and $\mu_{1,2}$ is the Jacobain matrix. Its eigenvalue equation can be obtained as $|m^{(1)}_{(d\times d)}m^{(2)}_{(d\times d)} - \varepsilon^2 e^{-2\lambda\delta}I| = 0$, where $m^{(k)}_{(d\times d)} = (\mu_k - (\lambda + \varepsilon e^{-\lambda\delta})I)$. The condition for the stability of the steady state for $\delta = 0$ can be deduced as $\varepsilon_{min} = \frac{\mu_1(\Delta - \mu_1)}{\Delta}$ when $d = 1$, where $\Delta = (\mu_1 + \mu_2)$ and hence the steady state is stable for $\varepsilon > \varepsilon_{min}$. The processing delay promotes the

onset of a right boundary $\varepsilon_{max} = \frac{1}{r_2}(r_1 \pm \sqrt{r_1^2 - 4\Delta(6-\delta\Delta)r_2})$, where $r_2 = 4\delta(48+24\delta\Delta+6\delta^2\Delta^2+\delta^3\Delta^3)$, $r_1 = (72+72\delta\Delta+3\delta^3\Delta(\Delta-2\mu)^2+\delta^4\Delta^2\mu(-\Delta+\mu)+12\delta^2(\Delta^2-3\Delta\mu+3\mu^2))$ provided $\delta<1$, beyond which the steady state is unstable. The stable region enclosed between the critical curves ε_{min} and ε_{max} diminishes on increasing δ as ε_{max} is a decreasing function of δ and finally disappears when $\varepsilon_{max} = \varepsilon_{min}$ at δ_c, thereby reviving the oscillations. Depending on the nature of the dependency of $\varepsilon_{max}/\varepsilon_{min}$ on the δ, either one or both of them approach each other and merge at δ_c to wipe out the AD/OD regions.

Now, we demonstrate that the processing delay can indeed evoke oscillations in AD/OD parameter space of the coupled chaotic systems. For this purpose, we have considered two coupled Sprott systems with a repulsive link represented as[16]

$$\dot{x}_i = -ay_i + \varepsilon_i(x_j(t-\delta) - x_i(t-\delta)), \tag{3a}$$

$$\dot{y}_i = x_i + z_i - \kappa_i(y_i(t-\delta) + y_j(t-\delta)), \tag{3b}$$

$$\dot{z}_i = x_i + y_i^2 - z_i, \tag{3c}$$

where $i,j = 1,2, i \neq j$, a is the system parameter, $\varepsilon = \varepsilon_2 = \kappa_1$ is the coupling strength, $\varepsilon_1 = \kappa_2 = 0$ contributes to the repulsive link, and δ is the processing delay. We have fixed $N=2$. The analog electronic circuit corresponding to system (3) and their evolution equations can be found in Ref. 30. The origin is the only unstable fixed point of the uncoupled system exhibiting chaotic oscillations for a wide range of a. In addition to the trivial fixed point at the origin, Eq. (3) has a nontrivial fixed point $x_1^* = z_1^*, y_1^* = 0, z_1^* = \frac{\varepsilon y_2^*}{2}, x_2^* = -z_2^*$, $y_2^* = \frac{(2a-\varepsilon^2)}{\varepsilon}, z_2^* = \frac{y_2^{*2}}{2}$. The origin is the HSS of the coupled system, while the other fixed point attributes to the IHSS.

Time evolution of the Sprott circuit systems is shown in Fig. 3 for $a=0.225$ and for different values of ε and δ. The stable HSS is depicted in Fig. 3(a) for $\varepsilon = 0.25$ until $\delta = 0$. The oscillations are revived instantaneously for the same coupling upon introducing the processing delay $\delta = 0.59$ at the instant indicated by the arrow. For the coupling strength $\varepsilon = 0.75$, the Sprott circuit systems exhibit the stable IHSS in the absence of the processing delay as shown in Fig. 3(b), which also elucidates that the oscillations are retrieved immediately for $\delta = 0.59$ even for the strength of the coupling conducive to onset of OD when $\delta = 0$. As the transition to death and reviving of oscillations from death are through a reverse Hopf and a Hopf bifurcations, respectively, the chaotic oscillations become limit-cycle oscillation through a reverse period-doubling just before death, and so the retrieved oscillations will also be periodic near δ_c.

The two parameter phase diagram of the Sprott circuit systems as a function of $\varepsilon \in (0,1)$ and $a \in (0.1, 0.4)$ is shown in Fig. 4(a) for a global perspective of the effect of the processing delay. The extent of the spread of the stable HSS (checked area) and that of the stable IHSS (shaded area) for different values of $\delta = 0, 0.33, 0.5, 0.59$, and 0.73 clearly reveals that the AD/OD regions shrink upon increasing the processing delay. Finally, above a critical value of

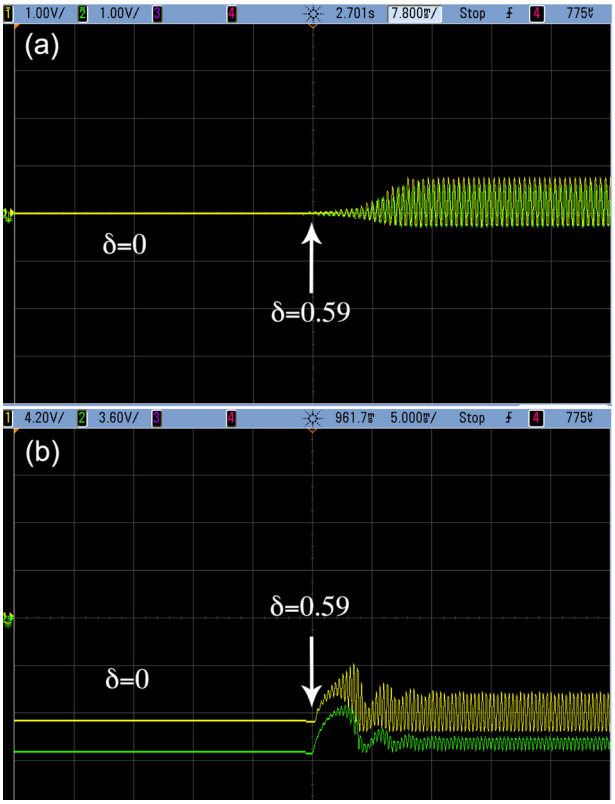

FIG. 3. Real time traces of the coupled Sprott oscillators (3) illustrating the revival of oscillation from the (a) AD state for $a = 0.225$ and $\varepsilon = 0.25$ as soon as the processing delay $\delta = 0.59$ is introduced in the coupling, and (b) OD state for $a = 0.225$ and $\varepsilon = 0.75$ upon introducing the processing delay $\delta = 0.59$ in the coupling.

$\delta, \delta_c = 0.78$, both stable HSS and stable IHSS lose their stability via a Hopf bifurcation reviving the natural rhythms of the coupled Sprott systems in the AD/OD parameter space.

The analytical stability curves of Eq. (3) demarcating the stable HSS and the stable IHSS are shown in Fig. 4(b) as a function of $\varepsilon \in (0, 1.2)$ and $a \in (0.2, 0.4)$. The critical

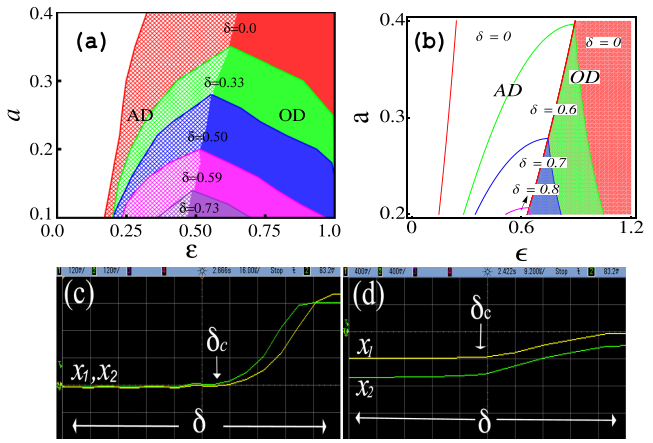

FIG. 4. Spread of the stable HSS and IHSS of the coupled Sprott oscillators (3) for different values of δ as a function of the coupling strength ε and the system parameter a elucidating the effect of the processing delay δ. (a) Experimental results and (b) analytical stability curves. Real time bifurcation diagrams elucidating the revival of oscillations for $\delta > \delta_c$ from (c) HSS for $a=0.225$, $\varepsilon = 0.25$ and (d) IHSS for $a=0.225$, $\varepsilon = 0.75$ as a function of the processing delay $\delta \in (0, 0.6)$.

curves encompassing the AD region of the coupled Sprott oscillators (3) before introducing the processing delay are deduced, by performing a linear stability analysis around the origin, as $a=(2-3\varepsilon^2-5\varepsilon^3-4\varepsilon^4-(1+\varepsilon)\sqrt{4+24\varepsilon+32\varepsilon^2-44\varepsilon^3-15\varepsilon^4+8\varepsilon^5+16\varepsilon^6})/(8(\varepsilon-1))$ (left boundary of AD) and $a=\frac{\varepsilon^2}{2}$ (right boundary of AD separating AD and OD). Similarly, the stability of the IHSS is ensured for $a>\frac{\varepsilon^2}{2}$. Now, to elucidate the effect of the processing delay, the critical curves in the presence of δ are determined after expanding $e^{-\lambda\delta}$ term in the characteristic equation of the coupled Sprott oscillators.[30] The critical stability curves for both AD and OD are depicted in Fig. 4(b) for different values of the processing delay $\delta=0,0.6,0.7,$ and 0.8. It is evident that the spread of AD/OD islands decreases for increasing δ and completely eroded above a critical value $\delta_c=0.86$ by switching the stability of the stable HSS and IHSS to revive the oscillations in the AD/OD regions confirming the experimental results in Fig. 4(a). Further, the real time bifurcation diagram of the coupled Sprott oscillators corroborates the revival of oscillations for $\delta>\delta_c$ from the AD state (see Fig. 4(c)) for $a=0.225$, $\varepsilon=0.25$ and from the OD state (see Fig. 4(d)) for $a=0.225$, $\varepsilon=0.75$ as a function of the processing delay $\delta\in(0,0.6)$.

In summary, we have experimentally demonstrated the effect of processing delay using analog electronic circuits of two coupled VDP and Sprott oscillators exhibiting limit cycle and chaotic oscillations, respectively. It has been shown that the processing delay is capable of shrinking the AD/OD regions and can eventually completely wipe off the AD/OD regions by switching the stability of the stable HSS/IHSS above a critical value. The phenomenon of reviving of oscillation is demonstrated in both the coupled VDP and Sprott circuit systems in the parameter space where AD to OD transition occurs as a function of the coupling strength. We have also obtained the analytical critical curves encompassing the stable HSS/IHSS as a function of the processing delay. Our analytical results also corroborate the effect of the processing delay in annihilating the onset of stable HSS/IHSS above a critical value of δ. The robustness of the phenomenon of reviving of oscillations by the processing delay is also verified for $N=100$ oscillators in both the coupled VDP and Sprott oscillators using simulations. Thus, the presence of even a small processing delay in the coupling results in retaining the natural rhythms of real world systems. The processing delay is particularly predominant in networks with large hubs and may be responsible for their dynamic robustness despite the presence of the couplings that can facilitate the onset of quenching of oscillations. We firmly believe that our results will open up the possibility of designing more robust technological networks, human-machine interfaces, etc., by the introduction of the processing delay in their circuit architecture.

D.V.S. was supported by the SERB-DST Fast Track scheme for young scientist under Grant No. ST/FTP/PS-119/2013. K.S. acknowledges the DST, India, and the Bharathidasan University for financial support under the DST-PURSE programme. The work of V.K.C. was supported by the INSA young scientist project. W.Z. acknowledges the financial support from the National Natural Science Foundation of China under Grant No. 11202082. K.T. acknowledges the DST, India, for financial support. S.K.D. was supported by the CSIR Emeritus scientist scheme.

[1]A. Pikovsky, M. Rosenblum, and J. Kurths, *Synchronization: A Universal Concept in Nonlinear Sciences* (Cambridge University Press, Cambridge, 2001).
[2]S. Boccaletti, J. Kurths, G. Osipov, D. L. Valladares, and C. Zhou, Phys. Rep. **366**, 1 (2002).
[3]Y. Kuramoto, *Chemical Oscillations, Waves, and Turbulence* (Springer, Berlin, 1984).
[4]W. L. Koukkari and R. B. Sothern, *Introducing Biological Rhythms* (Springer, Berlin, 2006).
[5]M. Lakshmanan and D. V. Senthilkumar, *Dynamics of Nonlinear Time-Delay Systems* (Springer, Berlin, 2010).
[6]G. Saxena, A. Prasad, and R. Ramaswamy, Phys. Rep. **521**, 205 (2012).
[7]A. Koseska, E. Volkov, and J. Kurths, Phys. Rep. **531**, 173–199 (2013).
[8]J. W. S. Rayleigh, *The Theory of Sound, Vol. 2* (Dover Publications, 1945); M. Abel, K. Ahnert, and S. Bergweiler, Phys. Rev. Lett. **103**, 114301 (2009).
[9]K. Bar-Eli, Physica D **14**, 242 (1985).
[10]G. B. Ermentrout and N. Kopel, SIAM J. Appl. Math. **50**, 125–146 (1990).
[11]B. F. Kuntsevich and A. N. Pisarchik, Phys. Rev. E **64**, 046221 (2001); A. Prasad, Y. C. Lai, A. Gavrielides, and V. Kovanis, Phys. Lett. A **318**, 71 (2003); M. Y. Kim, R. Roy, J. L. Aron, T. W. Carr, and I. B. Schwartz, Phys. Rev. Lett. **84**, 088101 (2005).
[12]D. V. R. Reddy, A. Sen, and G. L. Johnston, Phys. Rev. Lett. **85**, 3381–3384 (2000).
[13]I. Ozden, S. Venkataramani, M. A. Long, B. W. Connors, and A. V. Nurmikko, Phys. Rev. Lett. **93**, 158102 (2004).
[14]A. Koseska, E. Volkov, and J. Kurths, Phys. Rev. Lett. **111**, 024103 (2013).
[15]C. R. Hens, O. I. Olusola, P. Pal, and S. K. Dana, Phys. Rev. E **88**, 034902 (2013).
[16]C. R. Hens, P. Pal, S. K. Bhowmick, P. K. Roy, A. Sen, and S. K. Dana, Phys. Rev. E **89**, 032901 (2014).
[17]W. Zou, D. V. Senthilkumar, A. Koseska, and J. Kurths, Phys. Rev. E **88**, 050901(R) (2013); W. Zou, D. V. Senthilkumar, J. Duan, and J. Kurths, *ibid.* **90**, 032906 (2014).
[18]T. Banerjee and D. Ghosh, Phys. Rev. E **89**, 052912 (2014); **89**, 062902 (2014); D. Ghosh, T. Banerjee, and J. Kurths, *ibid.* **92**, 052908 (2015).
[19]M.-D. Wei and J.-C. Lun, Appl. Phys. Lett. **91**, 061121 (2007).
[20]D. Kondor and G. Vattay, PLoS One **8**, e57653 (2013).
[21]E. Ullner, A. Zaikin, E. I. Volkov, and J. García-Ojalvo, Phys. Rev. Lett. **99**, 148103 (2007); A. Koseska, E. Ullner, E. Volkov, J. Kurths, and J. García-Ojalvo, J. Theor. Biol. **263**, 189 (2010).
[22]K. Konishi, Phys. Lett. A **341**, 401–409 (2005); K. Morino, G. Tanaka, and K. Aihara, Phys. Rev. E **88**, 032909 (2013).
[23]A. Majdandzic, B. Podobnik, S. V. Buldyrev, D. Y. Kenett, S. Havlin, and H. E. Stanely *et al.*, Nat. Phys. **10**, 34–38 (2014).
[24]W. Zou, C. Yao, and M. Zhan, Phys. Rev. E **82**, 056203 (2010).
[25]W. Zou, D. V. Senthilkumar, and J. Kurths, Phys. Rev. Lett. **111**, 014101 (2013).
[26]D. V. Ramana Reddy, A. Sen, and G. L. Johnston, Phys. Rev. Lett. **80**, 5109 (1998).
[27]W. Zou, D. V. Senthilkumar, R. Nagao, I. Z. Kiss, Y. Tang, A. Koseska, J. Duan, and J. Kurths, Nat. Commun. **6**, 7709 (2015).
[28]A. Szucs, P. Varona, A. R. Volkovskii, H. D. I. Abarbanel, M. I. Rabinovich, and A. I. Selverston, Neuroreport **11**(3), 563 (2000).
[29]$b_c=(-4\varepsilon^3-2\varepsilon^4+40\varepsilon^5+20\varepsilon^6-136\varepsilon^7-48\varepsilon^8+219\varepsilon^9+25\varepsilon^{10}-193\varepsilon_{11}+29\varepsilon^{12}+118\varepsilon^{13}-22\varepsilon^{14}-63\varepsilon^{15}-5\varepsilon^{16}+18\varepsilon^{17}+6\varepsilon^{18})(-1-\varepsilon+2\varepsilon^2+21\varepsilon^4+43\varepsilon^5-119\varepsilon^6-183\varepsilon^7+318\varepsilon^8+328\varepsilon^9-526\varepsilon^{10}-300\varepsilon^{11}+514\varepsilon^{12}+162\varepsilon^{13}-258\varepsilon^{14}-70\varepsilon^{15}+54\varepsilon^{16}+18\varepsilon^{17})-1$.
[30]See supplementary material at http://dx.doi.org/10.1063/1.4947081 for analog circuits, circuit equation, normalized equation, and analytical procedures.